

# ALUMINOTHERMIC-CARBOTHERMAL REDUCTION SYNTHESIS OF NANO CRYSTALLINE $Al_2O_3$ -Ti(C,N) COMPOSITE WITH DIFFERENT BED TYPES

M. Heydari Nasab<sup>1</sup>, R. Naghizadeh<sup>2,\*</sup>, H. Samadi<sup>1</sup> and A. Nemati<sup>3</sup>

\* rnaghizadeh@iust.ac.ir

Received: June 2014

Accepted: December 2014

<sup>1</sup> Department of Material Engineering, Science and Research Branch, Islamic Azad University, Tehran, Iran.

<sup>2</sup> School of Metallurgy & Materials Engineering, Iran University of Science and Technology, Tehran, Iran.

<sup>3</sup> Department of Material Science and Engineering, Sharif University of Technology, Tehran, Iran.

**Abstract:** Ceramic-matrix composites containing TiC-TiN have been used in a variety of application because of their superior properties such as high hardness, good wear resistance and high chemical stability. In this research, effect of coke and coke/calcium beds in synthesis of  $Al_2O_3$ -Ti(C, N) composites using alumino-carbothermic reduction of  $TiO_2$  has been investigated. Al,  $TiO_2$  and active carbon with additives of extra carbon and NaCl and without additives, in separate procedures, have been mixed. Afterwards, mixtures were pressed and synthesized in 1200°C for 4hrs, in coke and coke/calcium beds, separately.  $Al_2O_3$ -Ti(C,N) composite was synthesized in ternary system of Al-TiO<sub>2</sub>-C with excess carbon and NaCl additives in calcium/coke bed in 1200 °C. X-ray diffraction patterns (XRD) results showed that existence of calcium in bed resulted in intensification of reduction atmosphere in samples and formation of Ti(C,N) phase enriched from carbon was accelerated. Crystallite sizes of synthesis Ti(C,N) at 1200 °C in reducing conditions were 22-28 nm.

**Keywords:** Alumino carbothermic reduction, Synthesis, Additives, Titanium carbonitride, Calcium/coke bed.

## 1. INTRODUCTION

Among ceramics, alumina, one of the first materials, has been used as cutting tools. However, low fracture toughness and relatively bad thermal shock resistance limit their applications. To modify these imperfections, alumina based composites such as alumina/titanium carbide or titanium nitride, alumina/silicon carbide whiskers and alumina/zirconia composites were produced [1]. Titanium carbide has significant properties such as hardness (28-35 Gpa), high chemical resistance, high melting point (3140 °C), suitable thermal conductivity (21w/m<sup>2</sup>k) and high strength. Addition of TiC to alumina can improve its toughness, hardness, and resistance to thermal shock and cracking. Compared to carbides like WC, titanium carbide has higher hardness (33%), higher thermal stability and lower density [1-3]. Also, titanium nitride has high melting point (2950 °C), good hardness (21Gpa), high chemical and thermal stability, and good thermal conductivity [2]. Addition of TiN to alumina-based composites improves their mechanical and

thermal properties. Titanium carbonitride, Ti(C,N) is a solid solution of TiC and TiN which has 0-1 mole carbon and shows properties of both TiC and TiN [4-7]. It is also more stable against molten steel than TiC and more applicable in coatings and cutting tools industrial. Xiang et al. [7] used mechanochemical process to mixture of aluminum powder and anatase and amorphous carbon to synthesize  $Al_2O_3$ -Ti(C, N) composite. Their process consists of 40 hrs high-energy milling in Ar/N<sub>2</sub> atmosphere and heat treatment in vacuum tube furnace at 1100 °C. In this study, homogeneous and fine  $Al_2O_3$ -Ti(C,N) composite powders from alumino carbothermic reduction of  $TiO_2$  in coke and coke/calcium beds were produced. Applying calcium in bed develops a new route for carbothermic reduction of oxides and formation of carbides.

## 2. EXPERIMENTAL

The starting materials for preparation of  $Al_2O_3$ -Ti(C,N) composite were Al powder (Merck, 98% purity), titania(Merck, 99% purity, anatase type), active carbon (Merck, 98% purity), novalak resin

and NaCl. Stoichiometric amount of Al powder, titania and active carbon, according to Eq. 1, were mixed and milled in dry ball mill for 60min using alumina balls.

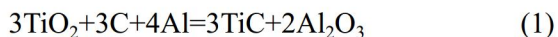


Table 1 shows percentage of raw materials of each sample beside their bed. Sample AB has stoichiometric amount of materials according to Eq.1., while sample AS has NaCl as additive and sample AC has 10%.wt additional active carbon. AS-K and AC-K samples were also embedded in coke/calcium bed.

As-prepared dry powders were mixed with novalak resin and aged for 4hrs in ambient condition and then pressed at 100 MPa pressure by uniaxial press. Disk shape samples ( $\Phi=20\text{mm}$ ) were heat treated in electrical furnace for 4hrs at 1200 in coke and coke/calcium beds in closed crucibles. Four string of calcium were

added to bed in coke/calcium bed route firing. The phase analyses of the powder samples were analyzed by “PANalytic X’Pert HighScore” using XRD patterns which were obtained with a Philips PW1800 diffractometer ( radiation,  $\lambda=0.154 \text{ nm}$ ) between  $2\theta=5-900$ . The average size of crystalline phases was estimated by X-ray line broadening technique employing Scherrer’s formula. To investigate morphology and size of particles, samples were subjected to TESCAN VEGAIXMU scanning electron microscope (SEM) which was equipped with energy-dispersive X-ray spectroscopy (EDS) for elemental analysis of samples. Fig. 1 shows flowchart of the process.

Fourier transform infrared spectrometer (FTIR) analysis was performed in  $400-4000 \text{ Cm}^{-1}$  range with Thermo Nicolet NeXus 870.Type of the chemical band and group of vibrating atoms can be identified via the ratio of absorption input infrared waves (I/I<sub>0</sub>).

**Table 1.** Composition of samples

Denotation	Additive	Bed	Al (wt. %)	TiO <sub>2</sub> (wt. %)	C (wt. %)	NaCl (wt. %)
AB	-	Coke	57.80	36.70	5.50	-
AS	NaCl	Coke	57.80	36.70	5.50	2
AC	Carbon	Coke	57.80	36.70	6.1	-
AS-K	NaCl	Coke+Ca	57.80	36.70	5.50	2
AC-K	Carbon	Coke+Ca	57.80	36.70	6.1	-

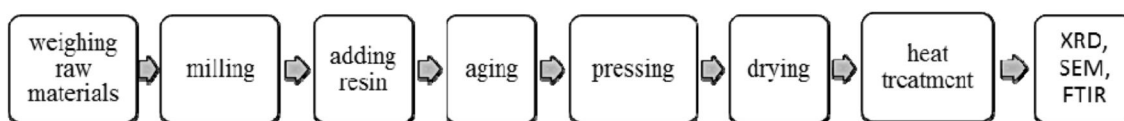


**Fig. 1.** Production and investigation stages of samples

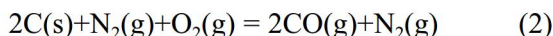


### 3. RESULTS AND DISCUSSION

#### 3. 1. XRD and Morphology Study

According to Fig. 2, showing XRD patterns of synthesized samples in coke bed, Al<sub>2</sub>O<sub>3</sub> (corundum), TiC or Ti(C,N) are major phases, and Al<sub>4</sub>C<sub>3</sub> and unreacted TiO<sub>2</sub> (rutile) are minor phases. Also unreacted Al can't be seen in XRD patterns in Fig. 2. Comparing Al<sub>4</sub>C<sub>3</sub> peaks in XRD patterns of three samples in Fig. 2 clarifies that AS and AC samples contain more Al<sub>4</sub>C<sub>3</sub> phases than AB sample.

The system is comprised of Al, TiO<sub>2</sub>, C, NaCl in the samples and CO and N<sub>2</sub> in surrounding atmosphere, which was resulted from reaction between air and coke bed according to Eq.2.



During heating of samples, Al melts at 870 °C, and splits of aluminum oxide layer are formed on

the surface of Al particles. Then molten Al spreads in the samples due to capillary suction action between particles. Two different mechanism reduced TiO<sub>2</sub> to sub-oxides of titanium oxide such as Ti<sub>3</sub>O<sub>5</sub>, TiO, TiO<sub>1-x</sub> and finally Ti. According to Richardson diagram, Al reduces TiO<sub>2</sub> to suboxides or Ti and converts to Al<sub>2</sub>O<sub>3</sub>. The second reduction mechanism of TiO<sub>2</sub> occurs due to reaction of CO(g) and solid carbon with TiO<sub>2</sub>. After reduction of TiO<sub>2</sub> to suboxides or Ti, formation of TiC or Ti(C,N) is accomplished. These reactions were shown in Eqs. 3-6. [8-9]

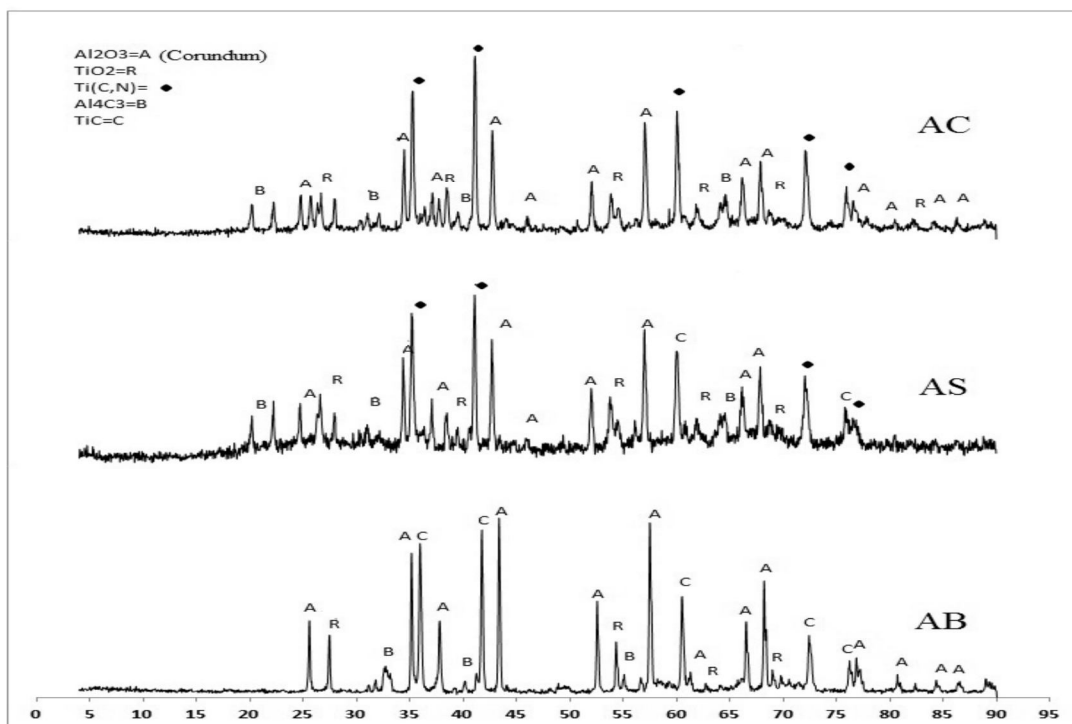
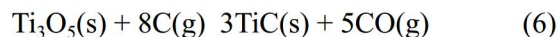
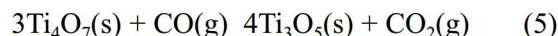
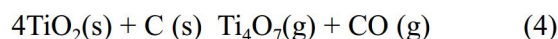


Fig. 2. XRD patterns of samples without and with 10% excess carbon and 2% NaCl additive in coke bed, synthesized in 1200 °C for 4hrs.

In sample without additives (AB sample),  $\text{Al}_2\text{O}_3$  and TiC were major phases, and rutile,  $\text{Al}_4\text{C}_3$  were minor phases.  $\text{TiO}_2$  (anatase) was transformed to TiC and unreacted  $\text{TiO}_2$  appeared as rutile phase. With addition of NaCl (AS sample), at firing temperature, molten alkali was formed and diffusion of different elements for formation of new phases was accelerated. Excess active carbon in (AC samples) increased contacts of  $\text{TiO}_2$  and solid carbon as well as the ratio of  $\text{CO}/\text{CO}_2$  around particles, so reduction reaction was accelerated.

In the system of Ti-Al-N, AlN,  $\text{Ti}_2\text{AlN}$  and  $\text{Al}_x\text{Ti}_y$  can be formed in nitrogen atmosphere [10-12] However, in the present research, formation of TiC, TiN, Ti(C,N), AlN and  $\text{Al}_4\text{C}_3$  is more probable due to existence of carbon in samples and CO,  $\text{N}_2$  in atmosphere. Absence of Ti(C,N) phase in samples without NaCl and excess carbon additives at 1200 reveals low rate of entrance of  $\text{N}_2$  in TiC lattice and formation of Ti(C,N). In formation procedure of Ti(C,N) from  $\text{TiO}_2$  [13], firstly TiON forms due to similar structural of TiN with TiO and then gradually changes to TiN or Ti(C,N) [13]. Formation of a sub-stoichiometric Ti(C,O) solid solution in some area of system with low pressure of  $\text{CO}(\text{g})$  also might be occurred. Then this intermediate compound gradually might be changed to Ti(C,O,N) and/or Ti(C,N). Ti(C,N) is a

solid solution of TiC and TiN in which TiN forms firstly and then C substitutes N. Increasing the amount of C in Ti(C,N) phase caused expansion of its lattice parameter, so the place of XRD peaks shifted. Structure of Ti(C, N) can be an ordered solid solution by XRD ref. number 00-042-1489. Addition of 2% of NaCl and 10% of excess carbon active resulted in appearance of Ti(C, N) peaks which are related to more formation of TiON and exchange of TiN to  $\text{TiC}_x\text{N}_{1-x}$ .

Fig. 3 shows XRD pattern of samples containing 2wt.% of NaCl (sample AS-K) and 10wt.% excess carbon active (sample AC-K) in coke plus calcium bed synthesized at 1200 . Existence of Ca is making atmosphere more reducing, so larger amount of  $\text{TiO}_2$  was reduced by Al or C(s) and  $\text{CO}(\text{g})$ . According to thermodynamic investigations, Ca absorbs more oxygen, while Ti absorbs more nitrogen [14]. Hence, more nitrogen from atmosphere penetrates into samples containing suboxides of titanium oxide such as TiO. Consequently, formation of TiON and then TiN and finally Ti(C,N) increases (Eqs. 7-9). Eq.7 shows that the reaction of air atmosphere ( $\text{O}_2/\text{N}_2$ ) with coke/calcium bed causes transformation of atmosphere of around samples to reduction state. Then  $\text{CO}(\text{g})$  and  $\text{N}_2(\text{g})$  diffused in samples ( $\text{TiO}_2+\text{Al}+\text{C}$ ) and different reactions such as

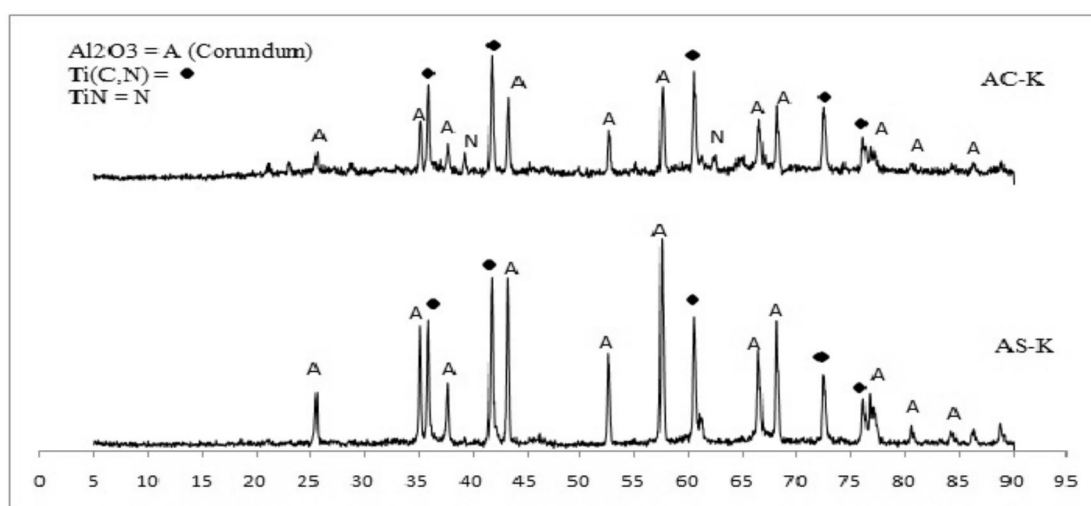
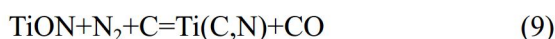
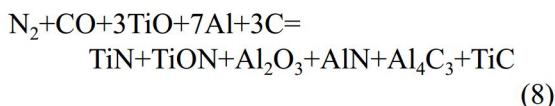
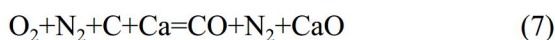


Fig. 3. XRD patterns of samples with 10% excess carbon and 2% NaCl in coke plus calcium bed, synthesized in 1200 for 4hrs.



aluminothermic, carbothermic and nitriding occur (Eq.8).



As can be seen in Fig. 4, Gibbs free energy determines that TiN is more stable than AlN [14]. Moreover, Fig. 5 indicates that establishment of TiC is more probable than Al<sub>4</sub>C<sub>3</sub> [15,16]. Even though Al<sub>3</sub>Ti can form in low ratio of C/Ti, it was not formed in our present research. From standpoint of Gibbs energy, formation of both TiC and Al<sub>x</sub>Ti<sub>y</sub> compositions have negative energy but TiC is more stable than Al<sub>x</sub>Ti<sub>y</sub> [15,16]. Also existence minor/negligible amount of Al<sub>4</sub>C<sub>3</sub> in some samples such as (AS) could be related to inhomogeneity of raw materials mixture or inadequate heating time.

was calculated based on Eq. 10. [16], where  $\alpha$ ,  $\lambda$ ,  $(hkl)$ , are lattice parameter, the wavelength of Cu K $\alpha$  ( $\lambda = 0.15406$  nm), plane indice and position of peak in the pattern respectively. Planes of (111), (200), (220) and (311) at angles ( $\theta$ ) 36.18, 42.02, 60.93 and 72.96 respectively were utilized to calculate the average ( $\alpha$ ) for Ti(C,N) in different samples as shown in Table 2. Amount of dissolved carbon in Ti(C<sub>x</sub>N<sub>1-x</sub>) determined from Eq. 11. [16, 17], Where ( $\alpha$ ) and ( $x$ ) are lattice parameter and mole fraction of dissolve carbon, respectively. Calculated lattice parameter of pure TiN and TiC are 0.424 nm and 0.4329 nm, respectively. Thus, dissolving of TiC in TiN results in increase of lattice parameter of Ti(C,N). The calculation of dissolved mole fractions of carbon in Ti(C<sub>x</sub>N<sub>1-x</sub>) indicates that the amount of dissolve carbon in Ti(C,N) were increased as shown in (AS-K and AC-K) samples toward to AS and AC, respectively with addition of calcium to bed. This is consequence of the increase in reduction condition around of samples and the conversion of CO<sub>(g)</sub> to C<sub>(s)</sub>+CO<sub>2(g)</sub> in inside of samples.

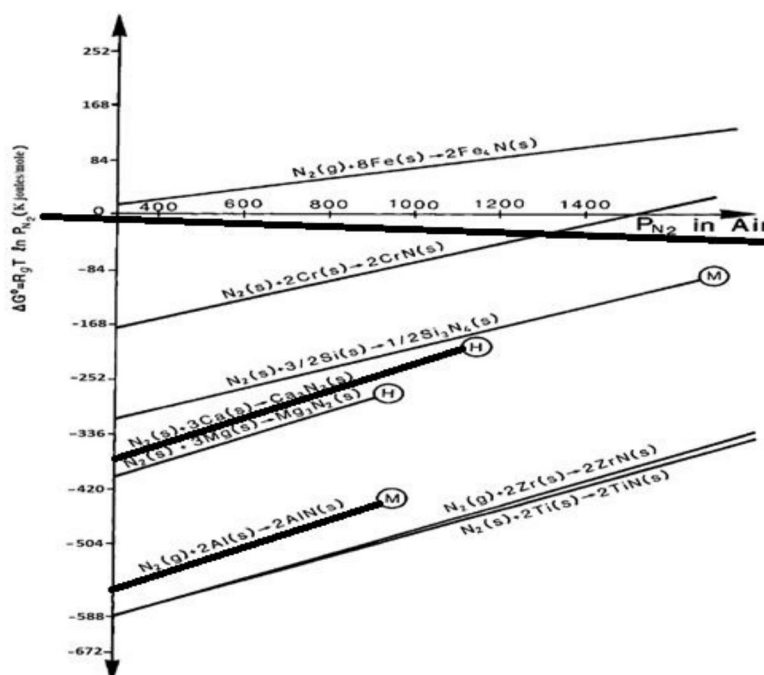


Fig. 4. Standard energy of formation of phases as a function of temperature [14]

Lattice parameter of Ti(C,N) in each sample

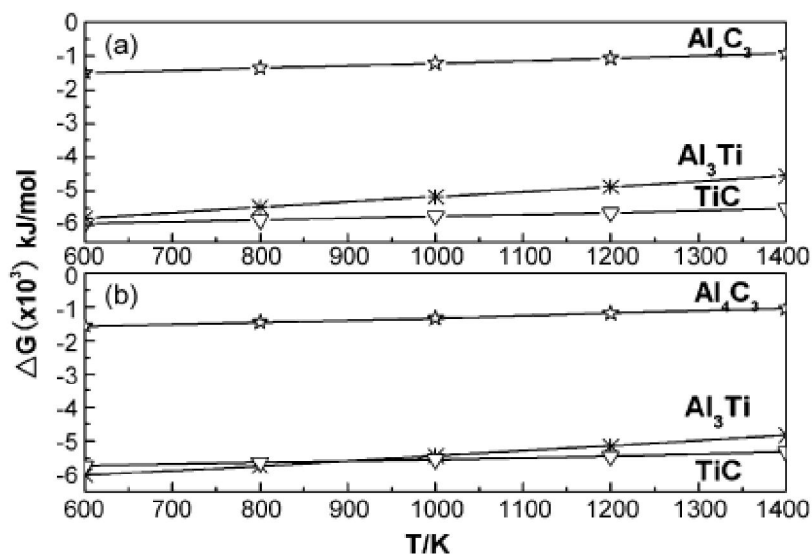


Fig. 5. Variation in the Gibbs free energy of TiC, Al<sub>3</sub>Ti and Al<sub>4</sub>C<sub>3</sub> with temperature at C/Ti (ratio)= 1.0, (a) 30wt.% Al and (b) 40wt.% Al.[15]

$$\alpha = \frac{\lambda(\sqrt{h^2 + k^2 + l^2})}{2 \sin \theta} \quad (10)$$

$$\alpha = 0.4235 + 0.007x \text{ (nm)} \quad (11)$$

Crystallite sizes of Ti(C,N) phase in different samples were calculated using XRD patterns and Sherrer equation (Eq.12), where D, λ, B, θ, are crystallite size(nm), wavelength of X-ray (λ=0.15406 nm), full width at half maximum (FWHM, rad) and position of peak in the pattern(rad), respectively [16].

$$D = \frac{0.9 \lambda}{B \cos \theta} \quad (12)$$

Calculated crystallite sizes of Ti(C,N) was 22-28 nm in all samples fired at 1200 °C in reducing condition.

### 3. 2. Microstructure Investigation

Fig. 6 depicts SEM micrograph of Al<sub>2</sub>O<sub>3</sub>-Ti(C,N) synthesized composite powder after firing at 1200 °C for 4hrs, in coke plus calcium bed (AS-K). Cuboid and globular particles (bright points) of Ti(C,N) are dispersed in Al<sub>2</sub>O<sub>3</sub> (dark point) matrix. Fig. 7 shows EDS analysis of AS-K sample at two different points.

According to XRD patterns and EDS analysis, corundum is matrix phase (dark areas) and Ti(C,N) with size of 0.5-1 μm (agglomerated in some part)

Table 2. Lattice parameter and mole fraction of carbon in Ti(C,N) established at different samples

Sample code	Ti(C,N) lattice parameter (nm)	Carbon amount
AS	0.4308	0.042
AC	0.4318	0.185
AS-K	0.4329	0.342
AC-K	0.4327	0.314

is reinforcement phase (bright points). It is clear that particle size of  $TiO_2$  and amount of NaCl salt melt at firing temperature have major effect on the particle size and shape of  $Ti(C,N)$ . It seems that  $TiON$  and  $TiN$  nucleate from surface of  $TiO_{1-x}$  suboxide and then carbon reached to surface from solid active carbon or molten NaCl that saturated from carbon. After formation of  $Ti(C,N)$  shell in surface, the reduction is controlled by diffusion of  $N_{2(g)}$ ,  $CO_{(g)}$  to the core of particles. Enhancement of reducing condition caused diffusion of  $CO_{(g)}$  to accelerate.

### 3. 3. FTIR Analysis

FTIR analysis was employed to study chemical bonds of samples. Fig. 8 shows infrared reflections of AC-K and AS-K samples. The broad absorption peak with high intensity in Fig. 8 from 500 to 1000  $Cm^{-1}$  is attributed to the characteristic absorption band of alumina and according to [18] resulting from the stretching of Al-O. Besides, its broad width is due to distribution of vacancies in octahedral and tetrahedral positions. Furthermore, according to

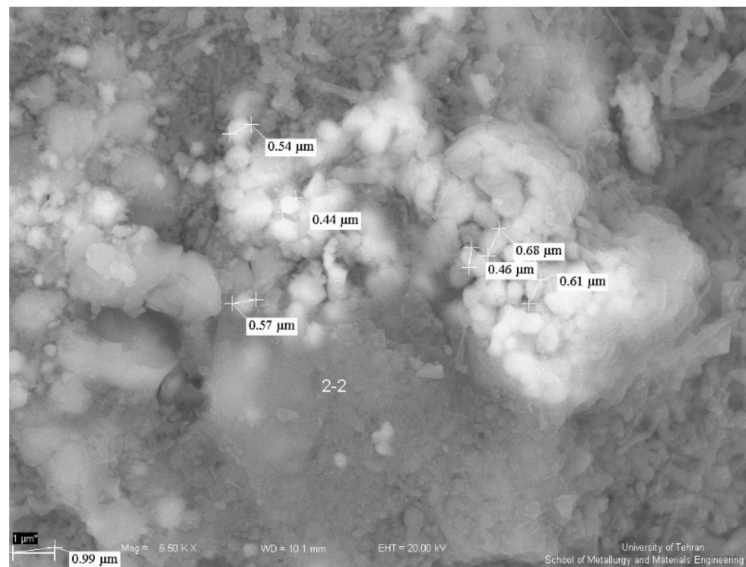


Fig. 6. FE-SEM of AS-K sample, 6500x magnification

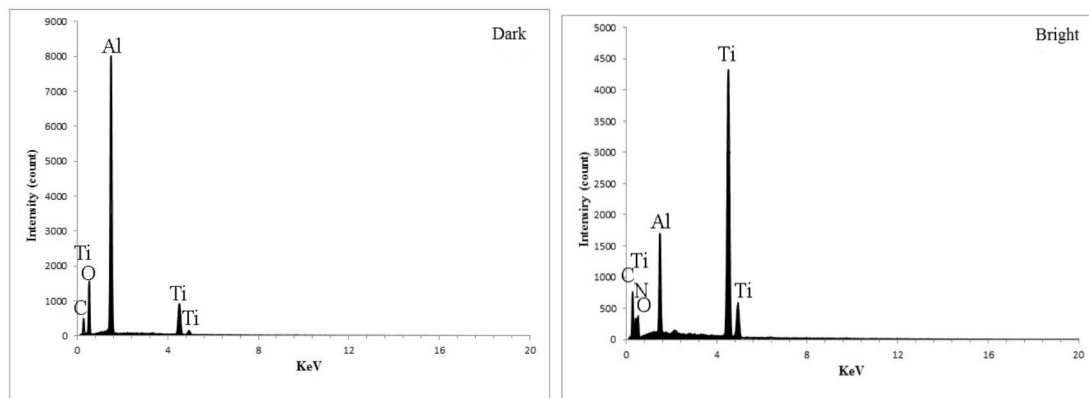


Fig. 7. EDS analysis of AS-K sample



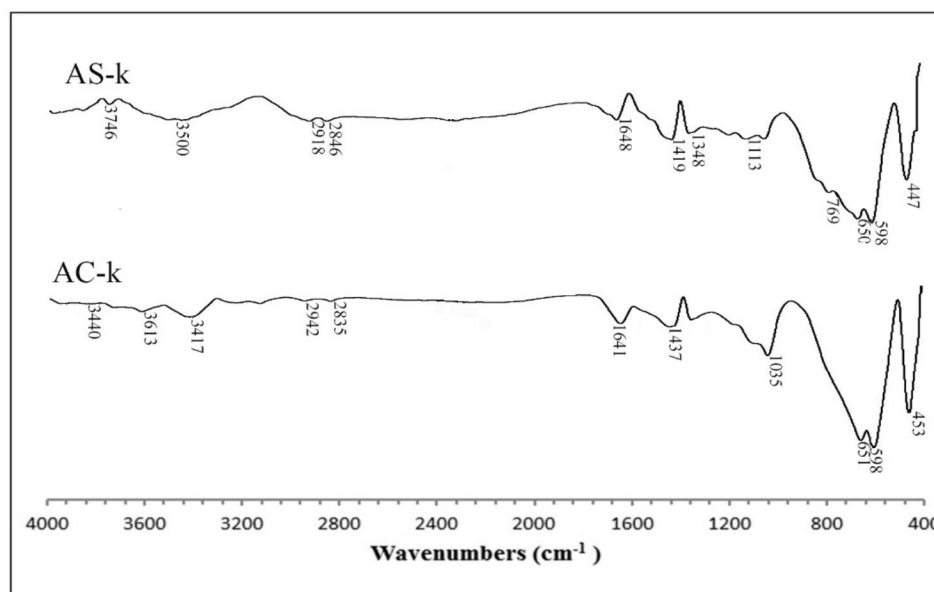


Fig. 8. Ft-IR spectrum of AC-K and AS-K samples.

[18], there are three characteristic peaks for alumina in 11385, 1124, 1628  $\text{Cm}^{-1}$  which can be seen in present research with slight shifting. As said by [19,20] chemical bonds of Ti-N, Ti-O-Ti and one of Ti-C peaks are overlapping in wavelengths lower than 500  $\text{Cm}^{-1}$ . According to these references Ti-N peaks is nearly at 480  $\text{Cm}^{-1}$ . The most important difference between Ti-N and Ti-O-Ti peak is that more oxygen and less nitrogen make peaks wider, as it can be seen in Fig. 8 that the peak in as mentioned area is sharp and narrow. As stated by [21] Ti-C is also retains three characteristic peaks in 270, 450 and 650  $\text{Cm}^{-1}$ . 270  $\text{Cm}^{-1}$  is out of range of device, 450  $\text{Cm}^{-1}$  is overlapping with Ti-N peak and 650  $\text{Cm}^{-1}$  is in the range of broad stretching peak Al-O. The adsorption peak near 1640  $\text{cm}^{-1}$  of two samples might be related to C=N or C=O bonds. The weak adsorption peak around 1340  $\text{cm}^{-1}$  is possibly related to C-N bonds with cross-linked structure.

#### 4. CONCLUSIONS

Composite powder of Ti(C,N) or  $\text{Al}_2\text{O}_3$ -TiC plus minor quantity of rutile phase and  $\text{Al}_4\text{C}_3$  in ternary system of  $\text{TiO}_2$ -Al-C, in coke bed and at 1200 °C was obtained. It is concluded that addition of diffusion accelerator (NaCl) and extra Carbon

are not beneficial in omitting the mentioned minor phases. Moreover, composite powder of  $\text{Al}_2\text{O}_3$ -Ti(C,N) was synthesized using carbothermic reduction of alumina in ternary system of Al-TiO<sub>2</sub>-C with extra carbon and NaCl in Ca/coke bed at 1200 °C. Microstructure of samples revealed that particles of Ti(C,N) are mostly agglomerated and cubic with the approximate size of 0.55 μm in alumina matrix. Crystallite size of Ti(C,N) is 24-27 nm.

#### 5. REFERENCES

1. Woo, Y. Ch., Kang, H. J., Kim, D. J., "Formation of TiC particle during carbothermal reduction of  $\text{TiO}_2$ ", Journal of the European Ceramic Society 27 (2007) 719-722
2. Ma, J., Wu, M., Duc, Y., Chen, S., Li, G., Hu, J., "Synthesis of nanocrystalline titanium nitride at low temperature and its thermal stability", journal of alloys and compounds 476(2008) 603-605
3. A. Amikaveei, A. Saidi, "Production of TiAl/Ti<sub>2</sub>AlC/ $\text{Al}_2\text{O}_3$  Composites by explosion synthesis", IJMSE, 9(4), (2012), 52-58
4. Jingguo Li, Lian Gao, Jingkun Guo "Mechanical properties and electrical conductivity of TiN- $\text{Al}_2\text{O}_3$  nanocomposites" journal of the European



- Ceramic Society 23 (2003) 69-74
5. Xilai Chen, Yuanbing Li, Yawei Li, Jiong Zhu, Shengli Jin, Lei Zhao, Zhongxing Lei, Xueqin Hong. (2007). "Carbothermic reduction synthesis of Ti(C, N) powder in the presence of molten salt, *Ceramics International*, 34, (2008), 1253-1259
  6. Fazelnajafabadi, M., Golzar, M. A., "In situ fabrication of Al-TiC composites by slag", *IJMSE*, 1(2), (2004), 9-12.
  7. Xiang, D. P., Liub, Y., Tub, M. J., Lia, Y. Y., Xiab, S., Chenb, B. Q., "Mechanochemical synthesis of ultrafine Ti(C,N)-Al<sub>2</sub>O<sub>3</sub> composite powders and phase transformation", *Journal of alloys and compounds* 473, (2009), 453-457
  8. Razavi, M., Rahimpour, M. R., & Kaboli, R. "Synthesis of TiC nanocomposite powder from impure TiO<sub>2</sub> and carbon black by mechanically activated sintering". *Journal of Alloys and Compounds*, 460(1), (2008), 694-698.
  9. Woo, Y. C., Kang, H. J., & Kim, D. J., "Formation of TiC particle during carbothermal reduction of TiO<sub>2</sub>", *Journal of the European Ceramic Society*, 27(2), (2007), 719-722.
  10. Lu, Q., Hu, J., Tang, K., Deng, B., Qian, Y., Zhou, G., & Liu, X. "The co-reduction route to TiC nano crystallites at low temperature", *Chemical physics letters*, 314(1), (1999), 37-39.
  11. Rond, B., Ramos, V. P. S., Ahmed, A. S., "The Role of Carbon in refractories", *IJMSE*, 1(3), (2004), 9-15.
  12. Chen, X., Li, Y., Li, Y., Zhu, J., Jin, S., Zhao, L., and Hong, X. "Carbothermic reduction synthesis of Ti (C, N) powder in the presence of molten salt", *Ceramics International*, 34(5), (2008), 1253-1259.
  13. Khosh Omid, E., Naghizadeh, R., Rezaie, H. R., "Synthesis and Comparison of MgAl<sub>2</sub>O<sub>4</sub>-Ti(C,N) Composites using aluminothermic-carbothermal reduction and molten salts routes", *Journal of Ceramic Processing Research*, 14(4), (2013), 445-447.
  14. Noorzadeh dehkordi, E., Samimbanhashemi, H. R., Naghizadeh, R., Rezaie, H. R., Goodarzi, M., "Synthesis of aluminum nitride in a coke-calcium reduction bed using nitrogen of the air", *Ceramic International*, in press.
  15. Li, Y. X., Hu, J. D., Wang, H. Y., Guo, Z. X., "Thermodynamic and lattice parameter calculation of TiCx produced from Al-Ti-C powders by laser igniting self-propagating high-temperature synthesis", *Materials Science and Engineering: A*, 458(1), (2007), 235-239.
  16. Mohapatra, S., Kumar Mishra, D., Kumor, Singh, S., "Microscopic and Spectroscopic analysis of TiC powder synthesized by thermal plasma technique", *Pasador technology*, 237, (2013), 41-45
  17. Yuanbing, L., Nan, L., Guozhi, R., Jianwei, L., Xiaohui, L., "Effects of technical factors on MgAl<sub>2</sub>O<sub>4</sub>-TiN composites produced by aluminothermic reduction and nitridation", *Material and Designing*, 28 (7), (2005), 969-972
  18. Ghezelbash, Z., Ashouri, D., Mousavian, S., Ghandi, A. H., & Rahnama, Y. "Surface modified Al<sub>2</sub>O<sub>3</sub> in fluorinated polyimide/ Al<sub>2</sub>O<sub>3</sub> nanocomposites: Synthesis and characterization", *Bulletin of Materials Science*, 35(6), (2012), 925-931
  19. Oliveira, C., Gonçalves, L., Almeida, B. G., Tavares, C. J., Carvalho, S., Vaz, F., Escobar-Galindo, R., Henriques, M., Susano, M., & Oliveira, R., "XRD and FTIR analysis of Ti-Si-C-ON coatings for biomedical applications", *Surface and Coatings Technology*, 203(5), (2008), 490-494.
  20. Vaz, F., Ferreira, J., Ribeiro, E., Rebouta, L., Lanceros-Méndez, S., Mendes, J. A., Alves, E., Goudeau, Ph., Riviere, J.P., Riberio, F., Moutinjo, I., Pischow, K., & De Rijk, J. "Influence of nitrogen content on the structural, mechanical and electrical properties of TiN thin films", *Surface and Coatings Technology*, 191(2), (2005), 317-323.
  21. Mohapatra, S., Mishra, D. K., & Singh, S. K. "Microscopic and spectroscopic analyses of TiC powder synthesized by thermal plasma technique", *Powder Technology*, 237, (2013), 41-45